

ICNMM2012-73199

## CREEPING FLOW THROUGH MICROCHANNELS WITH INTEGRATED MICRO-PILLARS

**Ali Tamayol**

Mechatronic Systems Engineering,  
Simon Fraser University, Surrey, BC,  
Canada, V3T 0A3  
[ali\\_tamayol@sfu.ca](mailto:ali_tamayol@sfu.ca)

**Naga S. K. Gunda**

Department of Mechanical  
Engineering, University of Alberta,  
Edmonton, AB, Canada, T6G 2G8  
[nagasiva@ualberta.ca](mailto:nagasiva@ualberta.ca)

**Mohsen Akbari**

Mechatronic Systems Engineering,  
Simon Fraser University, Surrey, BC,  
Canada, V3T 0A3  
[maa59@sfu.ca](mailto:maa59@sfu.ca)

**Sushanta K. Mitra**

Department of Mechanical  
Engineering, University of Alberta,  
Edmonton, AB, Canada, T6G 2G8  
[sushanta.mitra@ualberta.ca](mailto:sushanta.mitra@ualberta.ca)

**Majid Bahrami**

Mechatronic Systems Engineering,  
Simon Fraser University, Surrey, BC,  
Canada, V3T 0A3  
[mbahrami@sfu.ca](mailto:mbahrami@sfu.ca)

### ABSTRACT

Pressure drop through micro-pillar-integrated mini/microchannels is studied experimentally and analytically. Following our previous studies, the low aspect ratio micro-pillars embedded in a microchannel are modeled as a porous medium sandwiched between channel walls. The pressure drop is expressed as a function of the salient geometrical parameters such as channel dimension, diameter and spacing between the adjacent cylinders as well as their arrangement. To verify the developed model, several silicon/glass samples with and without integrated pillars are fabricated using the deep reacting ion etching (DRIE) technique. Pressure drop measurements are performed over a range of water flow rates ranging from 0.1 ml/min to 0.5 ml/min. The proposed model is successfully verified with the present experimental data. A parametric study is performed by employing the proposed model, which shows that the flow resistance has a reverse relationship with the micro-pillar diameter and the mini/microchannel porosity. In addition, staggered arrangements have a significantly lower flow resistance than squared arrays of pillars especially in dense structures.

**Keywords:** Microchannels; Porous media; Pressure drop; Brinkman equation

### NOMENCLATURE

$d$	=	Cylinder diameter, $m$
$E(\cdot)$	=	Uncertainty associated with measured parameters
$h$	=	Channel depth, $m$
$K$	=	Permeability, $m^2$
$L$	=	Channel length, $m$

$P$	=	Pressure, $N/m^2$
$Q$	=	Volumetric flow rate ( $\mu l/min$ )
$Re$	=	Reynolds number
$S$	=	Distance between centers of adjacent cylinders, $m$
$U$	=	Volume averaged velocity, $m/s$

### Greek symbols

$\varepsilon$	=	Porosity
$\mu$	=	Viscosity, $N.s/m^2$
$\mu_{eff.}$	=	Effective viscosity, $N.s/m^2$
$\mu'$	=	Viscosity ratio, $\mu' = \mu_{eff.} / \mu$

### INTRODUCTION

Mini/microchannels with integrated micro-pillars offer enhanced heat and mass transfer coefficients, surface-area-to-volume ratio, and thermal conductance in comparison with plain microchannels. Thus, they have been used for an array of applications such as microreactors [1, 2], micro heat exchangers [3-5], micro-total analysis systems ( $\mu$ TAS) [6], micropumping [7, 8], and microfilters [9]. However, the integrated micro-pillars increase the shear force exerted to the passing fluid which results in a pressure drop augmentation. Determining the optimum design for the arrays of micro-pillars requires an accurate model that can predict the pressure drop as a function of the salient geometrical parameters of the micro-pillar-integrated-microchannel assembly.

The creeping flow across ordered arrays of infinitely long cylinders has been the subject of numerous studies; see for example references [10-14]. According to the experimental results reported by Kosar et al. [3], Vanapalli et al. [15], and Yeom et al. [16], employing the existing models for long cylinders may lead to a significant inaccuracy in the analysis of

flow through low aspect ratio cylinders embedded inside mini/microchannels. Therefore, a more general model should consider the channel walls' effects in the analysis in order to successfully predict the flow through the cylinder array. In two recent studies, Tamayol et al. [17, 18] successfully employed two different approaches for analyzing creeping flow through minichannels filled with square arrays of micro-cylinders: i) porous medium approach in which the assembly was modeled as a channel filled with a porous medium; ii) variable cross-section channel approach, where the flow between cylinders was modeled as the flow along a variable cross-section microchannel. They also performed a comprehensive experimental study for creeping through 15 silicon samples [18]. Comparison of the two models with the experimental data showed that that the variable cross-section approach is more accurate for dense structures but it fails for samples with high porosity. The porous medium approach on the other hand was more flexible and in a reasonable agreement with experimental data over a wide range of porosity [18]. In spite of the existing studies reviewed here, the effects of the important geometrical parameters such as pillar arrangement and porosity are not fully understood. This present study aims at providing a better understanding of such relations.

Following Tamayol et al. [18], the low aspect ratio micro-pillars embedded in a microchannel are modeled as a porous medium sandwiched between channel walls. The Brinkman equation is used to predict the overall pressure drop, where permeability of the porous medium is evaluated from the model proposed by Tamayol et al. [19] previously.

To determine the accuracy of the developed model, an independent experimental study is carried out. For this reason, several samples of mini/microchannels filled with arrays of micro-cylinders, covering a range of geometric parameters, are fabricated using the deep reaction ion etching (DRIE) method. Pressure drop of the samples is measured over a range of volumetric flow rates. The comparison shows that the model captures the trend observed in experimental data over the entire range of cylinder spacing and diameter.

## PROBLEM FORMULATION

### Tested samples

The studied geometry, shown in Figure 1, is comprised of repeating square and staggered arrangements of mono disperse cylinders, embedded in a constant cross-section rectangular microchannel. It has been stated in the literature that the fully developed condition is achieved within the first 3 rows of cylinders in the creeping flow regime; see for example [20]. Therefore, the entrance effects are neglected in the present study. In addition, the flow is assumed to be steady state, incompressible and fully developed with constant fluid properties. Moreover, non-continuum effects such as slip flow are neglected in the analysis [21, 22].

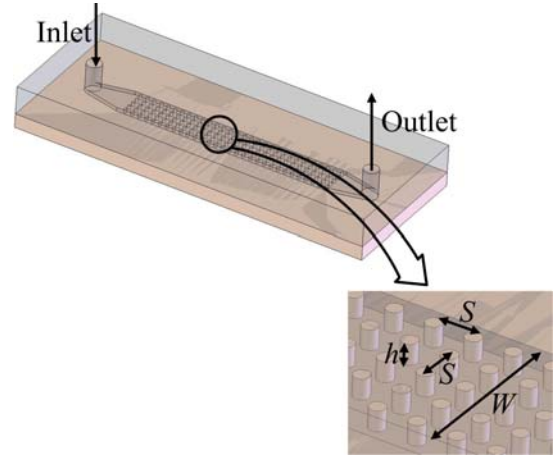


Figure 1: Structure of the considered microchannels filled with arrays of micro-cylinders.

### Porous medium approach

In low Reynolds number flows through porous media, the relationship between the applied pressure drop and the volume averaged (superficial) velocity is linear and can be described by the Darcy equation [23]:

$$-\frac{dP}{dx} = \frac{\mu}{K} U \quad (1)$$

where  $\mu$  is the fluid viscosity and  $K$  is the permeability of the medium. For analyzing flow through confined porous media, an additional term should be added to the right hand side of Eq. (1) to satisfy the no-slip boundary condition on solid walls, which leads to the Brinkman equation [24]:

$$-\frac{dP}{dx} = \frac{\mu}{K} U + \mu_{eff} \frac{d^2 U}{dy^2} \quad (2)$$

where  $\mu_{eff}$  is the effective viscosity [23, 24]. The exact value of the viscosity ratio  $\mu' = \mu / \mu_{eff}$  for various porous media is not clearly known in the literature [25]. However, Tamayol et al. [17] have shown that the model of Ochoa-Tapia and Whitaker [26], which uses  $\mu' = 1/\varepsilon$  is an accurate assumption for arrays of cylinders; where  $\varepsilon$  is the porosity of the porous medium.

Tamayol et al. [17] also demonstrated that for channels with small aspect ratios, i.e.,  $\varepsilon' = h/W < 0.1$ , the problem can be envisioned as a porous medium sandwiched between two parallel plates, as shown in Figure 2. Therefore, the pressure drop,  $\Delta P$ , calculated from Eq. (2) becomes [17]:

$$\frac{\Delta P}{L} = \frac{\mu Q \sinh\left(\frac{h}{\sqrt{\mu' K}}\right)}{K h \left[ 2 \frac{\sqrt{\mu' K}}{h} \left[ -1 + \cosh\left(\frac{h}{\sqrt{\mu' K}}\right) \right] - \sinh\left(\frac{h}{\sqrt{\mu' K}}\right) \right]} \quad (3)$$

$$, \mu' = 1/\varepsilon$$

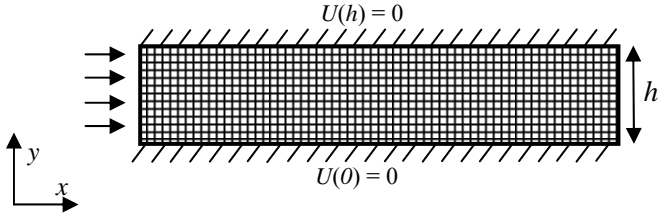


Figure 2: Schematic of the simplified 2D geometry.

To calculate the pressure drop from Eq. (3), one needs to know the permeability,  $K$ . Depending upon the microstructure of the porous medium, various relationships exist for the calculation of the permeability; see for example [19, 23, 27-30].

The permeability of infinitely long cylinders in ordered arrangements for flow normal to their axes has been studied extensively in the literature [10-14]. Recently, Tamayol and Bahrami [19] employed a scale analysis technique and developed an analytical model for permeability of cylindrical fibers in various arrangements. Their model for dimensionless permeability of square and staggered arrangements of fibers provides:

$$\frac{K}{d^2} = \begin{cases} \frac{0.16 \left[ \frac{\pi}{4\phi} - 3\sqrt{\frac{\pi}{4\phi}} + 3 - \sqrt{\frac{4\phi}{\pi}} \right]}{\sqrt{1-\phi}} & \text{Square} \\ \frac{0.16 \left[ \frac{\pi}{2\sqrt{3}\phi} - 3\sqrt{\frac{\pi}{2\sqrt{3}\phi}} + 3 - \sqrt{\frac{2\sqrt{3}\phi}{\pi}} \right]}{\sqrt{1-\phi}} & \text{Staggered} \end{cases} \quad (4)$$

where  $d$  is the diameter of the cylinders, as shown in Figure 1, and  $\phi$  is the solid volume fraction determined from:

$$\phi = 1 - \varepsilon = \begin{cases} \frac{\pi d^2}{4S^2} & \text{Square} \\ \frac{\pi d^2}{2\sqrt{3}S^2} & \text{Staggered} \end{cases} \quad (5)$$

where  $S$  is the distance between adjacent cylinders and  $\varepsilon$  is the porosity of the arrangement. In the present study, Eq. (4) is used to calculate the permeability of the cylinders embedded inside the microchannels.

## EXPERIMENTAL INVESTIGATION

### Microfabrication

The silicon (Si) microchannels filled with an array of micro-pillars were created using the standard MEMS fabrication techniques to verify the trend of the proposed analytical model. Several samples with and without integrated micro-pillar were designed and fabricated to demonstrate the effect of porosity, cylinder arrangement, and channel depth on the flow resistance. The diameters of micro-cylinders range from 30 to 100  $\mu\text{m}$ , and the micro-cylinders spacing ranges from 81 to 135  $\mu\text{m}$ , covering a wide range of porosity from 0.5 to 0.90. The geometrical parameters of all the samples are summarized in Table 1. The channel's name in

Table 1 indicates the cylinder arrangement, intended porosity, and the expected cylinders diameter. For example, Sq-0.50-100 corresponds to square arrangement, porosity of 0.5 with cylinders of 100  $\mu\text{m}$ . The permeability of the embedded porous media, calculated from Eq. (4) is also listed in

Table 1. In addition, two microchannels without micro-pillars were fabricated to calibrate the experimental setup and determine the depth of the fabricated samples.

The fabrication procedure of the microchannels with an array of micro-cylinders was reported elsewhere [16] but briefly described here. A 100-mm-diameter Si wafer (Silicon Valley Microelectronics Inc., Santa Clara, CA) was taken and cleaned with Piranha solution. Then, a 0.5 micron thick oxide layer was deposited on top of it. After that microchannels with integrated micro-pillars are patterned on silicon/silicon-dioxide wafer with standard photolithography using HPR506 (Fuji-film Electronic Materials Inc., Mesa, Arizona) positive photoresist (PPR). Subsequently oxide and silicon layers are anisotropically etched in plasma-reactive ion etchers. After etching the silicon for about  $\sim 100 \mu\text{m}$ , the PPR on the wafer was stripped off using acetone and the wafer was thoroughly cleaned in Branson PPR stripper. Then oxide layer was removed using HF dip. Then 1.1-mm-thick, 100 mm square borofloat glass wafer was used as covering layer for the microchannels. Inlet and outlet ports are drilled on glass covering layer using abrasive water-jet cutter (2652 Jet Machining Center, OMAX, Kent, WA). Anodic bonding of patterned silicon wafer with glass covering layer has been done using, SUSS bonder after cleaning both wafers in piranha solution. The microscopic image of some of the fabricated micro-pillars embedded inside a microchannel is shown in Figure 3.

### Test setup

The open loop system, illustrated in Figure 4, was employed for measuring the steady pressure drop in the fabricated samples. A syringe pump (Harvard Apparatus, QC, Canada) was employed to provide a user-specified flow rate to the system with a controlled flow rate of 0.5% accuracy. Distilled water was flown through a submicron filter before entering the minichannel. To measure the pressure drop, a gauge pressure transducer (Omega Inc., Laval, QC, Canada) was fixed at the channel inlet while the channel outlet was discharged to the atmosphere. Teflon tubing (Scientific Products and Equipment, North York, Canada) was employed to connect the pressure transducer to the syringe pump and the microchannel. Pressure drops were measured for several flow rates in the range of 50-800  $\mu\text{l}/\text{min}$  ( $8.3-103 \times 10^{-10} \text{ m}^3/\text{s}$ ).

The viscous dissipation effect is neglected in this study; thus, the properties of the flowing water are considered to be constant. The connecting pressure loss is measured directly at each flow rate when the end of the tubing is disconnected from the sample. To perform accurate measurements, the level of the tubing end should be identical to the case where the samples are connected; this prevents any error due to hydrostatic pressure difference. Moreover, Akbari et al. [31] showed that the developing pressure drop and the minor pressure losses in microchannels are less than 1% of the total pressure loss; thus, can be neglected.

The uncertainty of the analysis is mostly a result of the uncertainty in the fabrication process and the uncertainty in the channel and cylinder size measurements. A calibrated optical microscope was used to record the channel and micro-cylinder dimensions. Five independent measurements were obtained for each sample and the average values were used in the analysis. In addition, the uncertainty of the measured values of flow resistance in various trials and flow rates for each sample, included in the plots, was calculated as follows [32]:

$$\frac{E(\Delta P/Q)}{(\Delta P/Q)} = \sqrt{\left(\frac{E(\Delta P)}{\Delta P}\right)^2 + \left(\frac{E(Q)}{Q}\right)^2} \quad (6)$$

where  $E(\cdot)$  indicates the uncertainty associated with the involved parameters. The uncertainty in the measured values is less than 10%.

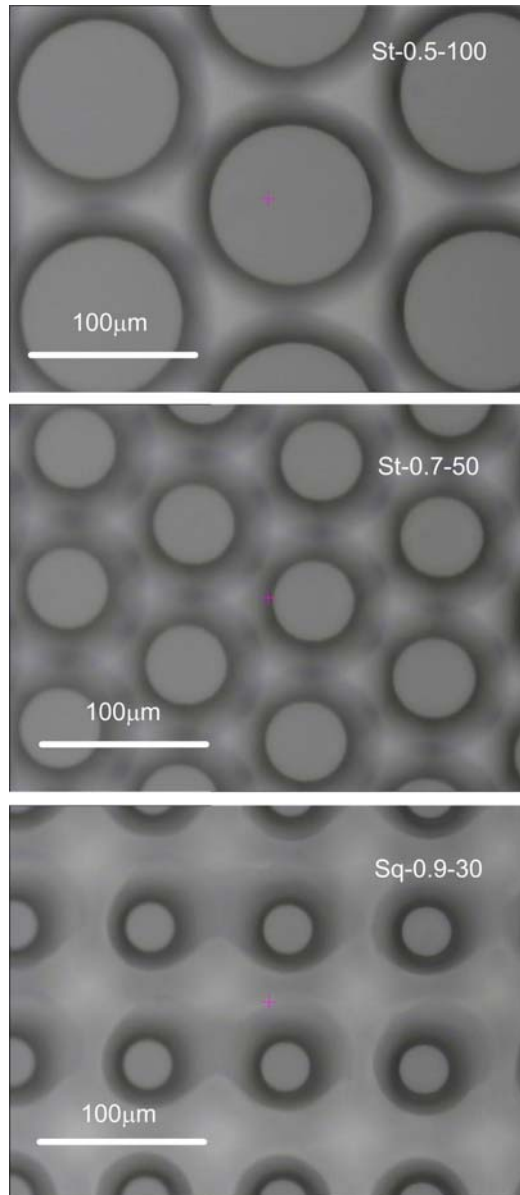


Figure 3: Microscope images of some fabricated micro-cylinder arrays in silicon.

## RESULTS AND DISCUSSION

The microchannels with and without integrated micro-pillars were fabricated simultaneously on the same silicon chip. The fabricated microchannels were tested first to ensure the accuracy of the experimental procedure. In Figure 5, the experimental values of flow resistance,  $\Delta P/(\mu LU)$ , are compared with the theoretical values calculated using the model of Shah and London [33] for fully developed flow through rectangular channels. It can be seen that the data and the model are in a good agreement. These results also confirm the accuracy of measurements of the channel dimensions.

The values of flow resistance obtained by the developed model, Eq. (3) and (4), are compared with the present experimental data in Figure 6 for some of the tested samples. Consistent with the creeping flow assumption, it can be seen that the experimental values of  $\Delta P/(\mu LU)$  almost remain constant over the investigated range of flow rates. In addition, it can be seen that the agreement between the proposed model and the experimental data is reasonable. It should be noted that channel depth, spacing between cylinders, and their diameter affect the overall pressure drop.

Once validated, the proposed model, Eq. (3) and (4), can be used to investigate the effect of micro-pillar arrangement on the flow resistance of the microchannels with integrated cylinders. For this purpose, a typical channel with a constant width of  $2000 \mu m$  and depth of  $100 \mu m$  is assumed. Moreover, two micro-pillar sets with diameters of  $10 \mu m$  and  $50 \mu m$  are considered in the analysis. As can be seen from Figure 7, there is an inverse relationship between the porosity and the flow resistance. At a constant porosity (the same surface-to-volume-ratio), square arrangements samples have a higher flow resistance. This deviation is more pronounced in lower porosities where the difference between permeability values calculated by Eq. (4) is more significant. In addition, the results suggest that the use of smaller pillars lead to a much higher flow resistance.

## SUMMARY AND CONCLUSIONS

Pressure drop through arrays of micro-pillar embedded inside mini/microchannels was studied both experimentally and analytically. The assembly was modeled as a porous medium sandwiched between parallel plates and a compact relationship was proposed for the pressure drop as a function of the channel geometrical parameters such as width/height, diameter and the spacing between the adjacent cylinders as well as their arrangement. Several silicon/glass samples with and without integrated pillars were fabricated using the deep reacting ion etching (DRIE) technique. Pressure drop measurements were performed over a range of water flow rates and the results were used to validate the developed model. Moreover, a parametric study was conducted, which can be summarized as follows:

- Flow resistance had a reverse relationship with both porosity and pillar diameter
- Staggered arrays of micro-pillar resulted in a lower pressure drop in comparison with the square counterparts at the same porosity

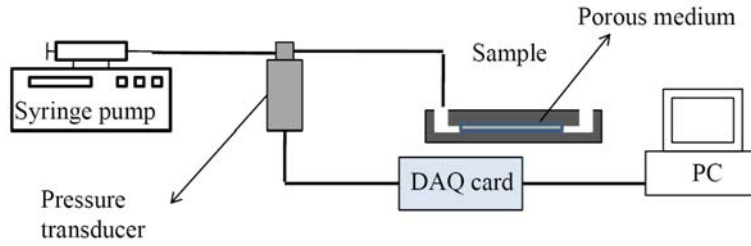


Figure 4: Schematics of the designed experimental setup.

Table 1: Geometrical properties of the fabricated samples. The channel's name in the table indicates the cylinder arrangement, intended porosity, and the expected cylinders diameter.

Sample	$S (\mu m)$	$K (m^2)$	$W (\mu m)$	$h (\mu m)$	$L (mm)$
Sq-0.5-100	125	$2.84 \times 10^{-11}$	1250	94	18.87
Sq-0.7-50	81	$7.03 \times 10^{-11}$	808	94	24.46
Sq-0.8-50	99	$2.13 \times 10^{-10}$	990	94	34.45
Sq-0.9-30	84	$2.99 \times 10^{-10}$	841	94	37.13
St-0.5-100	135	$6.13 \times 10^{-11}$	1346	91	20.11
St-0.7-50	87	$9.59 \times 10^{-11}$	869	91	24.26
St-0.8-50	106	$2.97 \times 10^{-10}$	1064	91	33.05
St-0.9-30	90	$4.05 \times 10^{-10}$	900	91	37.72
Channel 1	--	--	841	94	38.70
Channel 2	--	--	900	91	39.67

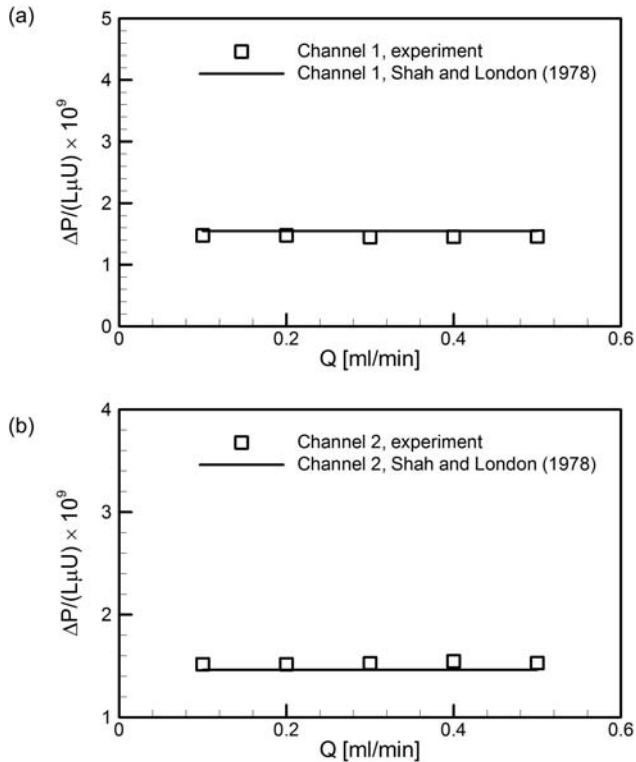


Figure 5: Comparison of flow resistance versus flow rate for channels without integrated micro-pillar with the model of Shah and London [33].

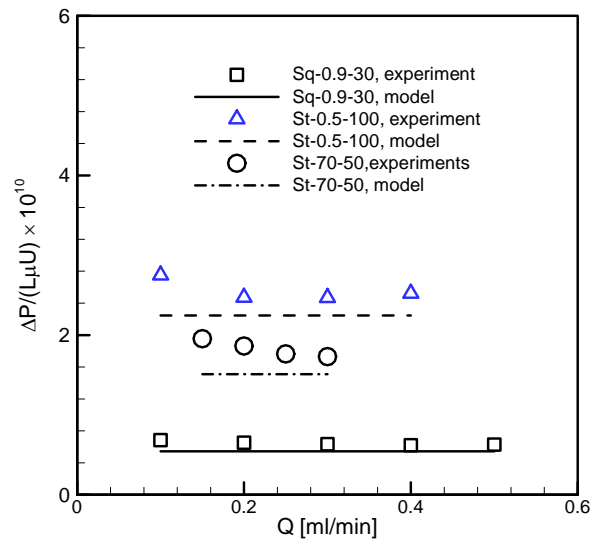


Figure 6: Flow resistance versus flow rate for samples Sq-0.9-30, St-0.5-100, and St-0.7-50. Symbols show the experimental data; lines present the values predicted by the proposed model, Eq. (3).

## ACKNOWLEDGEMENTS

Financial support of Natural Science and Engineering Research Council (NSERC) of Canada is gratefully acknowledged. A.T. and M.A. thank British Columbia Innovation Council (BCIC) for financial support through Innovation Scholar awards. The

authors gratefully acknowledge the financial support of Alberta Innovates – Technology Futures, in the form of a scholarship for N.S.K.G.

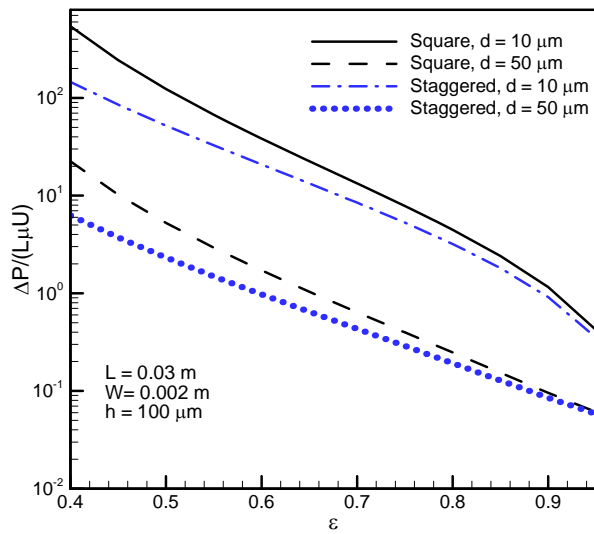


Figure 7: Experimental values of flow resistance versus the values predicted by the proposed model, Eqs. (3) and (4).

## REFERENCES

[1] M. Roumanie, C. Pijolat, V. Meille, C. De Bellefon, P. Pouteau, C. Delattre, Deposition of Pt-catalyst in a microchannel of a silicon reactor: Application to gas micro-TAS working at high temperature, *Sensors and Actuators B: Chemical*, 118(1-2) (2006) 297-304.

[2] M.W. Losey, R.J. Jackman, S.L. Firebaugh, M.A. Schmidt, K.F. Jensen, Design and fabrication of microfluidic devices for multiphase mixing and reaction, *Journal of Microelectromechanical Systems*, 11(6) (2002) 709-717.

[3] A. Kosar, C. Mishra, Y. Peles, Laminar flow across a bank of low aspect ratio micro pin fins, *Journal of Fluids Engineering*, 127(3) (2005) 419-430.

[4] Y. Peles, A. Kosar, C. Mishra, C. J. Kuo, B. Schneider, Forced convective heat transfer across a pin fin micro heat sink, *International Journal of Heat and Mass Transfer*, 48(17) (2005) 3615-3627.

[5] A. Tamayol, A. Kholsa, B.L. Gray, M. Bahrami, Pressure drop in micro-channels filled with porous media, in: ICNMM2010, Montreal, Canada, 2010.

[6] S. Nagrath, L.V. Sequist, S. Maheswaran, D.W. Bell, D. Irimia, L. Ulkus, M.R. Smith, E.L. Kwak, S. Digumarthy, A. Muzikansky, P. Ryan, U.J. Balis, R.G. Tompkins, D.A. Haber, M. Toner, Isolation of rare circulating tumour cells in cancer patients by microchip technology, *Nature*, 450(7173) (2007) 1235-1239.

[7] A. Saha, S. Mitra, M. Tweedie, S. Roy, J. McLaughlin, Experimental and numerical investigation of capillary flow in SU8 and PDMS microchannels with integrated pillars, *Microfluidics and Nanofluidics*, 7(4) (2009) 451-465.

[8] A. Mathur, S.S. Roy, M. Tweedie, S. Mukhopadhyay, S.K. Mitra, J.A. McLaughlin, Characterisation of PMMA microfluidic channels and devices fabricated by hot embossing

and sealed by direct bonding, *Current Applied Physics*, 9(6) (2009) 1199-1202.

[9] Y. Yong-Kyu, P. Jung-Hwan, F. Cros, M.G. Allen, Integrated vertical screen microfilter system using inclined SU-8 structures, in: *Micro Electro Mechanical Systems, 2003. MEMS-03 Kyoto. IEEE The Sixteenth Annual International Conference on*, 2003, pp. 227-230.

[10] A. Tamayol, M. Bahrami, Analytical determination of viscous permeability of fibrous porous media, *International Journal of Heat and Mass Transfer*, 52(9-10) (2009) 2407-2414.

[11] M. Sahraoui, M. Kaviany, Slip and no-slip velocity boundary conditions at interface of porous, plain media, *International Journal of Heat and Mass Transfer*, 35(4) (1992) 927-943.

[12] J. Happel, Viscous flow relative to arrays of cylinders, *AIChE Journal*, 5(2) (1959) 174-177.

[13] A. Tamayol, M. Bahrami, Transverse permeability of fibrous porous media *Physical Review E*, (2010).

[14] J.E. Drummond, M.I. Tahir, Laminar viscous flow through regular arrays of parallel solid cylinders, *International Journal of Multiphase Flow*, 10(5) (1984).

[15] S. Vanapalli, H. J. M. ter Brake, H. V. Jansen, J. F. Burger, H. J. Holland, T. T. Veenstra, M.C. Elwenspoek, Pressure drop of laminar gas flows in a microchannel containing various pillar matrices, *Journal of Micromechanics and Microengineering*, 17(7) (2007) 1381.

[16] J. Yeom, D. D. Agonafer, J. H. Han, M.A. Shannon, Low Reynolds number flow across an array of cylindrical microposts in a microchannel and figure-of-merit analysis of micropost-filled microreactors, *Journal of Micromechanics and Microengineering*, 19(6) (2009) 065025.

[17] A. Tamayol, A. Kholsa, B.L. Gray, M. Bahrami, Creeping flow through ordered arrays of micro-cylinders embedded in rectangular minichannels, *International Journal of Heat and Mass Transfer*, In press (2011).

[18] A. Tamayol, J. Yeom, M. Akbari, M. Bahrami, Low Reynolds number flows across ordered arrays of micro-cylinders embedded in rectangular micro/minichannels, *International Journal of Heat and Mass Transfer*, Submitted (2012).

[19] A. Tamayol, M. Bahrami, Transverse permeability of fibrous porous media, *Physical Review E*, 83(4) (2011) 046314.

[20] W. Zhong, I. Currie, D. James, Creeping flow through a model fibrous porous medium, *Experiments in Fluids*, 40(1) (2006) 119-126.

[21] A. Tamayol, K. Hooman, Slip-flow in microchannels of non-Circular cross sections, *Journal of Fluids Engineering*, 133(9) (2011) 091202.

[22] M. Bahrami, A. Tamayol, P. Taheri, Slip-flow pressure drop in microchannels of general cross section, *Journal of Fluids Engineering*, 131(3) (2009) 031201.

[23] M. Kaviany, *Principles of Heat Transfer in Porous Media*, 2nd ed., Springer-Verlag, New York, 1995.

[24] H. C. Brinkman, A calculation of the viscous force exerted by a flowing fluid on a dense swarm of particles, *Applied Scientific Research*, 1(1) (1949) 27-34.

[25] A. Tamayol, K. Hooman, M. Bahrami, Thermal analysis of flow in a porous medium over a permeable stretching wall, *Transport in Porous Media*, 85(3) (2010) 661-676.

- [26] J. A. Ochoa-Tapia, S. Whitaker, Momentum transfer at the boundary between a porous medium and a homogeneous fluid-- I. Theoretical development, *International Journal of Heat and Mass Transfer*, 38(14) (1995) 2635-2646.
- [27] B. T. Astrom, R. B. Pipes, S.G. Advani, On flow through aligned fiber beds and its application to composites processing, *Journal of Composite Materials*, 26(9) (1992) 1351-1373.
- [28] A. Tamayol, M. Bahrami, In-plane gas permeability of proton exchange membrane fuel cell gas diffusion layers, *Journal of Power Sources*, 196(7) (2011) 3559-3564.
- [29] M. M. Tomadakis, T.J. Robertson, Viscous permeability of random fiber structures: comparison of electrical and diffusional estimates with experimental and analytical results, *Journal of Composite Materials*, 39(2) (2005) 163-188.
- [30] M. Akbari, D. Sinton, M. Bahrami, Laminar fully developed flow in periodically converging-diverging microtubes, *Heat Transfer Engineering*, 31(8) (2010) 628-634.
- [31] M. Akbari, D. Sinton, M. Bahrami, Pressure drop in rectangular microchannels as compared with theory based on arbitrary cross section, *Journal of Fluids Engineering*, 131(4) (2009) 041202-041201-041208.
- [32] J. R. Taylor, *An introduction to error analysis: The study of uncertainties in physical measurements*, Second ed., University Science Books,, Sausalito, USA, 1997.
- [33] R.K. Shah, A.L. London, *Laminar Flow Forced Convection in Ducts*, Academic Press,, New York, 1978.